

RESEARCH ARTICLE

Metagenome of a Microbial Community Inhabiting a Metal-Rich Tropical Stream Sediment

Patrícia S. Costa¹, Mariana P. Reis¹, Marcelo P. Ávila¹, Laura R. Leite², Flávio M. G. de Araújo², Anna C. M. Salim², Guilherme Oliveira², Francisco Barbosa¹, Edmar Chartone-Souza¹, Andréa M. A. Nascimento¹*

1 Departamento de Biologia Geral, Instituto de Ciências Biológicas, Universidade Federal de Minas Gerais, Belo Horizonte, Minas Gerais, Brazil, **2** Centro de Pesquisas René Rachou Fundação Oswaldo Cruz, Belo Horizonte, Minas Gerais, Brazil

* amaral@ufmg.br



OPEN ACCESS

Citation: Costa PS, Reis MP, Ávila MP, Leite LR, de Araújo FMG, Salim ACM, et al. (2015) Metagenome of a Microbial Community Inhabiting a Metal-Rich Tropical Stream Sediment. PLoS ONE 10(3): e0119465. doi:10.1371/journal.pone.0119465

Academic Editor: Zhili He, University of Oklahoma, UNITED STATES

Received: August 29, 2014

Accepted: January 29, 2015

Published: March 5, 2015

Copyright: © 2015 Costa et al. This is an open access article distributed under the terms of the [Creative Commons Attribution License](https://creativecommons.org/licenses/by/4.0/), which permits unrestricted use, distribution, and reproduction in any medium, provided the original author and source are credited.

Data Availability Statement: The nucleotide sequences were submitted to Sequence Read Archive (SRA, <http://www.ncbi.nlm.nih.gov/sra/>) with the accession number of SRR1573431.

Funding: This study was supported by FAPEMIG APQ 00801/12 and APQ-00463-13, CNPq nu472411/2012-8, CNPq/INCT no 15206-7. The funders had no role in study design, data collection and analysis, decision to publish, or preparation of the manuscript.

Competing Interests: The authors have declared that no competing interests exist.

Abstract

Here, we describe the metagenome and functional composition of a microbial community in a historically metal-contaminated tropical freshwater stream sediment. The sediment was collected from the Mina Stream located in the Iron Quadrangle (Brazil), one of the world's largest mining regions. Environmental DNA was extracted and was sequenced using SOLiD technology, and a total of 7.9 Gbp was produced. A taxonomic profile that was obtained by comparison to the Greengenes database revealed a complex microbial community with a dominance of *Proteobacteria* and *Parvarcheota*. Contigs were recruited by bacterial and archaeal genomes, especially *Candidatus Nitrospira defluvii* and *Nitrosopumilus maritimus*, and their presence implicated them in the process of N cycling in the Mina Stream sediment (MSS). Functional reconstruction revealed a large, diverse set of genes for ammonium assimilation and ammonification. These processes have been implicated in the maintenance of the N cycle and the health of the sediment. SEED subsystems functional annotation unveiled a high degree of diversity of metal resistance genes, suggesting that the prokaryotic community is adapted to metal contamination. Furthermore, a high metabolic diversity was detected in the MSS, suggesting that the historical arsenic contamination is no longer affecting the prokaryotic community. These results expand the current knowledge of the microbial taxonomic and functional composition of tropical metal-contaminated freshwater sediments.

Introduction

Prokaryotic species exhibit broad distribution, having been researched across a wide range of natural environments such as soil, marine and freshwater, as well as in plants, animals and humans. Many of these species have been revealed to be important for the health and/or ecological balance of various environments. Indeed, a link between the set of microbial species and the

host or environment-associated biological processes and health has been extensively reported [1, 2]. Because of their essential roles in life and in ecosystem functioning, ambitious multidisciplinary efforts across the globe are ongoing to characterize microbial communities [3].

Sediment has been recognized as a special realm in aquatic ecosystems because its species richness is higher than that of the water community and is comparable to soil microbial diversity [4, 5]. In mining-contaminated regions, sediments of water bodies play an important role in the transport and storing of contaminants. Indeed, sediment characteristics determine the ecological balance and biodiversity of the aquatic ecosystem [6].

There is a consensus in the literature that metal-contaminated freshwater sediment exhibits an extremely complex and well-adapted community [7–9]. These studies revealed that *Proteobacteria*, especially *Beta-proteobacteria*, and *Bacteroidetes* are the main contributors to the composition of these environments. It should be noted that sediment communities play an important role in biogeochemical cycling and are involved in the transformation of nutrients such as N and C [9].

Although previous studies of microbial communities in metal-contaminated freshwater sediment have been performed [5, 8, 10, 11], none of them assessed the microbial community of a metal-contaminated tropical sediment through taxonomic and functional diversity evaluation. Moreover, all of the studies, except Reis *et al.* [8], focused their analysis on sediments of temperate streams. However, due to the restricted power of the methodology employed by Reis *et al.* [8], these authors did not cover all of the taxonomic richness present in the tropical stream studied here. Thus, much is still unknown about the functional and taxonomic microbial diversity of tropical metal-contaminated streams. Considering that microorganisms play an essential role in environmental biogeochemical cycling, and may influence the speciation and bioavailability of metals, it is relevant to obtain a more comprehensive knowledge of the taxonomic and functional diversity of the prokaryotic community in metal-contaminated freshwater sediments.

One powerful strategy to assess both the functional and taxonomic microbial diversity is a metagenomic approach. Indeed, over the last 20 years, new sequencing technologies, together with metagenomic and computational tools, have transformed microbial ecology research. Metagenomics provides insight into the interactions of microbial communities with the environment and offers an extraordinary opportunity to comprehensively examine the ecosystem's response to environmental changes [12]. However, metagenomic surveys that thoroughly assess the microbial diversity in freshwater sediments with extreme geochemical conditions involving high concentrations of As, Fe, and Mn are still lacking.

In this study, we applied a shotgun metagenomic approach and a metabolic analysis to examine the taxonomic and functional composition of the prokaryotic community of a historically metal-contaminated tropical stream sediment. The stream studied herein, the Mina Stream, is located in the Iron Quadrangle (IQ, Brazil), one of the world's largest mining regions, which has been undergone to mining activities since the late 17th century. Accordingly, the IQ presents a historical metal contamination of waters and sediments from streams and rivers, including the Mina Stream [8, 13–16]. We also performed comparative metagenomic analysis between our metagenome and a rich arsenic well metagenomic dataset from Bangladesh [17].

Material and Methods

Ethics statement

For sampling in the Mina Stream, no specific permit was required for the described field study. The study location is not privately owned or protected in any way, and we confirmed that the field study did not involve endangered or protected species.

Study area

The Mina stream (19°58'46.80"S and 43°49'17.07"W) is located in one of the world's largest mining regions and is extremely rich in iron and gold ores (Iron Quadrangle, Minas Gerais state, Brazil). Collections of Mina stream sediment have been previously described by our group [11]. This stream was chosen because it has suffered stress by metal pollution exceeding the maximum allowable concentrations established by Brazilian environmental regulations, such as Cu 387.7 mg kg⁻¹, Zn 180.9 mg kg⁻¹ and As 297.1 mg kg⁻¹, which were presented in an earlier study [11].

The sediment sample in this study was taken from the upper part (oxic zone) during the dry season and was named according to the location from which it was retrieved, i.e., Mina Stream sediment (MSS). For metabolic analysis, the anaerobic environment of the sediment sample was maintained by substituting the O₂ for CO₂ using a CO₂ pump, and the tube was hermetically closed. Two hours after collection, the sediment sample was introduced into an anaerobic chamber where subsequent experiments were performed.

Microbial metabolic diversity

The capability of aerobic and anaerobic sediment microbial communities to utilize different carbon sources was assessed using Biolog Ecoplate (Biolog, Inc, Hayward, CA, USA). This system contained 31 carbon sources, in triplicate, divided into amines, amino acids, carbohydrates, carboxylic acids, and polymers, among others. In addition to the specific carbon source, each well contained tetrazolium violet redox dye as a color indicator for the utilization of the carbon sources by the microorganisms [18] (S2 Table). Sediment sample was filtered (10 g wet weight; pore size 0.45 μm) and diluted in sterile saline. Then, 120 μL from the 10⁻² dilutions was inoculated into each well and subsequently incubated aerobically and anaerobically in the dark at 28°C. Color development was measured at OD₅₉₀ every 24 h for 4 d using an ELISA plate reader (BIO-RAD Model 3550 Microplate Reader). For the anaerobic BIOLOG assay, four plates were used, one for each day of reading. This procedure was performed by taking into account the loss of anaerobic conditions when the plate was withdrawn from the anaerobic chamber. For aerobic conditions, one plate was used. The detected value of the absorbance for the blank (water) reading was subtracted from all wells.

Ecoplate data analysis

The data generated by 96 h readings were statistically analyzed. Because raw OD₅₉₀ values were corrected, the microbial activity for each microplate was expressed as the average well-color development (AWCD) and was calculated as follows: $AWCD = \sum OD_i / 31$ where OD_i is the optical density value for each well. The richness (number of carbon substrates consumed) and the Shannon-Weaver index were calculated using a cutoff line of OD = 0.25 for a positive microbial response [19]. The Shannon-Weaver index was calculated as follows: $H' = -\sum p_i (\ln p_i)$, where p_i is the ratio between the microbial activity of each substrate (OD_i) and the sum of microbial activities of all substrates (∑OD_i). The Evenness index was calculated with the formula $E = H' / \ln R$, where H' is the value of the Shannon index, and R is the richness of substrates.

DNA extraction and shotgun metagenomic sequencing

Total DNA was extracted from the sediment sample (10 g wet weight) using the PowerSoil DNA Extraction kit (MoBio Laboratories, USA) according to the manufacturer's instructions. Quantification and quality of total DNA were determined using the Agilent 2100 Bioanalyzer equipment according to the manufacturer's instructions.

Sediment sample was subjected to shotgun sequencing using the high-throughput sequencer Applied Biosystems SOLiD v.4 following the manufacturer's protocol. Briefly, 10 µg of total DNA was randomly fragmented using the Covaris S2 System. A DNA fragment library from 200 to 250 bp long was constructed for sequencing. Then, emulsion PCR was performed to clonally amplify fragments on sequencing beads, followed by enrichment and preparation for deposition in plate for sequencing according to the manufacturer's instructions (http://tools.lifetechnologies.com/content/sfs/manuals/SOLiD4_Library_Preparation_man.pdf). After sequencing, 50 bp reads were generated for further analysis.

16S rRNA gene amplification and sequencing

Amplification of the V3-V4 hypervariable region of the 16S rRNA gene was performed using region-specific bacterial/archaeal primers S-D-Bact-0341-b-S-17 forward 5'-CCTACGGGNGGCWGCAG-3' and S-D-Bact-0785-a-A-21 reverse 5'-GACTACHVGGG-TATCTAATCC-3' [20], with Illumina adapters added. Barcoded amplicons were generated using KAPA HiFi HotStart ReadyMix (KAPA, Woburn, MA, USA) and were purified using AMPure XP beads (Agencourt Bioscience, Beverly, MA, USA). Sequencing was performed using the MiSeq platform (Illumina, Inc., San Diego, CA, USA) according to the manufacturer's instructions (http://support.illumina.com/documents/documentation/chemistry_documentation/16s/16s-metagenomic-library-prep-guide-15044223-b.pdf).

Bioinformatics analysis

V3-V4 region from 16S rRNA gene. 16S rRNA microbiota primary data analysis was performed with PRINSEQ (stand alone lite version, <http://prinseq.sourceforge.net/>), where quality-based trimming was performed. Reads with N's or an overall mean Q-score of < 25 were discarded. The resulting fasta file was also screened for ambiguous bases and homopolymers using MOTHUR v.1.33.0 (<http://www.mothur.org>). Furthermore, chimeras were detected using the UCHIME algorithm (<http://drive5.com/uchime>).

Operational taxonomic units (OTUs) and taxonomic classification were determined using the MOTHUR pipeline [20, 21] and the Greengenes reference database (http://greengenes.secondgenome.com/downloads/database/13_5, from May 2013) to obtain the microbial composition of the MSS microbiota. OTUs were determined using similarity levels between sequences of at least 97% for classifying a microorganism at the species level, as proposed by Drancourt *et al.* [22]. Good's coverage [23] was calculated for OTUs with an evolutionary distance of 0.03. Rarefaction curves were calculated for OTUs with an evolutionary distance of 0.03, 0.05 and 0.10. The nucleotide sequences were submitted to Sequence Read Archive (SRA, <http://www.ncbi.nlm.nih.gov/sra/>) with the accession number of SRR1573431.

Shotgun metagenome data. Metagenomic primary data analysis was performed with SOLiD Accuracy Enhancement Tool (SAET) software (<http://solidsoftwaretools.com/gf>), a spectral alignment algorithm that screens for errors inherent to the sequencing platform and the encodeFasta.py program (<http://gnome.googlecode.com/svn/trunk/pyGenotypeLearning/src/pytools/encodeFasta.py>), that converts the sequences represented in color space to letter space format. Then, the assembly of the metagenome data was performed to generate contigs using the Metavelvet software [24] with parameters according to the recommendations of the authors (kmer 27,-exp_covauto) [24].

A Fasta file with contig sequences was deposited into the Metagenomics RAST Server (MG-RAST v3.3) [25]. Prior to annotation, MG-RAST provides a quality control of sequences that consists of artificially removing duplicate sequences and screening based on quality and size of sequences. Functional analysis was performed using the SEED subsystem and KEEG available

on MG-RAST with the following cutoff parameters: 1×10^{-5} e-value and 60% of identity percentage [26]. The data from this study are available via MG-RAST with the ID 4519449.3.

A recruitment plot was used to identify abundant species genomes in the MSS metagenome. In this representation, MSS metagenome contigs were compared to individual bacterial genomes. Fragment recruitment of the MSS contigs was performed using BLASTN against bacterial and archaeal complete genomes. Data were plotted using R (<http://cran.r-project.org>), and the criteria for counting a hit were a minimum identity of 90%, e-value cutoff 0.001 and minimum alignment of 50 bp.

Comparative metagenomic analysis. Comparative metagenomic analysis was performed using the Statistical Analysis of Metagenomic Profiles (STAMP) program [27] to determine statistically significant functional composition differences in any two metagenomes using two-sided Fisher exact tests [27]. The most important metabolic categories were selected by using a p-value >0.05 . To accomplish that, the MG-RAST functional matches at all levels were compared using the SEED database (<http://www.theseed.org>). The statistical comparison was conducted with the data from a rich arsenic well metagenome (4461675.3) [17] due to similarity between the two environments, i.e., the high As contamination.

Real-time PCR (qPCR)

Quantitative real-time PCR was performed to estimate the absolute number of copies of bacterial and archaeal 16S rRNA genes in the MSS. To accomplish this outcome, total DNA sample was added to a 20 μ l reaction containing a SYBR Green master mix and the bacterial and archaeal primer set: 338F (5'-TACGGGAGGCAGCAG-3') and 344F (5'-ACGGGGCGCAG-CAGGCGCGA-3'), respectively [28] and 518R (5'-ATTACCGCGGCTGCTGG-3') for both [29]. Standard curves were generated from the 16S rRNA gene amplicons obtained using conventional PCR from *Halococcus morrhuaea* ATCC 17082 and *Escherichia coli* ATCC 25922 as previously described by Cardinali-Rezende *et al.* [30]. The procedure was performed using the ABI PRISM 7900HT sequence detection system (Applied Biosystems, Foster City, CA). The conditions used to amplify the 16S rRNA gene from bacteria and archaea were according to Cardinali-Rezende *et al.* [30].

Results

Taxonomic composition of the prokaryotic community

The MSS microbiota resulted in 273,710 high-quality reads with an average read length of 450 bp. Of a total of 31,656 OTUs, 678 OTUs were not classified within the Bacteria and Archaea domains. Thus, a total of 30,978 OTUs remained for downstream analysis. Of these OTUs, 22,184 were singletons and 2,242 were doubletons composed of only a few reads (27,077). Bacteria were by far the most abundant prokaryotic domain, constituting 98.2% (30,738 OTUs), whereas archaeal reads showed a relative paucity (1.8%, 240 OTUs). The Good's coverage value (89%) and rarefaction curve (S1 Fig.) obtained with an evolutionary distance of 0.03 indicated that most of the prokaryotic diversity was detected in the sample.

Bacterial and archaeal phyla diversity are shown in Fig. 1 and S1 Table. A total of 30,738 OTUs were assigned to 52 known bacterial phyla. Nevertheless, most OTUs were affiliated with four phyla: *Proteobacteria* (45%), *Bacteroidetes* (18%), and an equal proportion (4%) of *Acidobacteria* and OD1. The group "other bacteria" comprised minor bacterial phyla such as *Gemmatimonadetes*, *Cyanobacteria*, *OP3*, *OP11*, *Spirochaetes*, and *TM7*, among others, representing 8% of the OTUs. Furthermore, 2,157 OTUs were considered to be unclassified at the phylum level and, thus, may represent new bacterial taxa (Fig. 1).

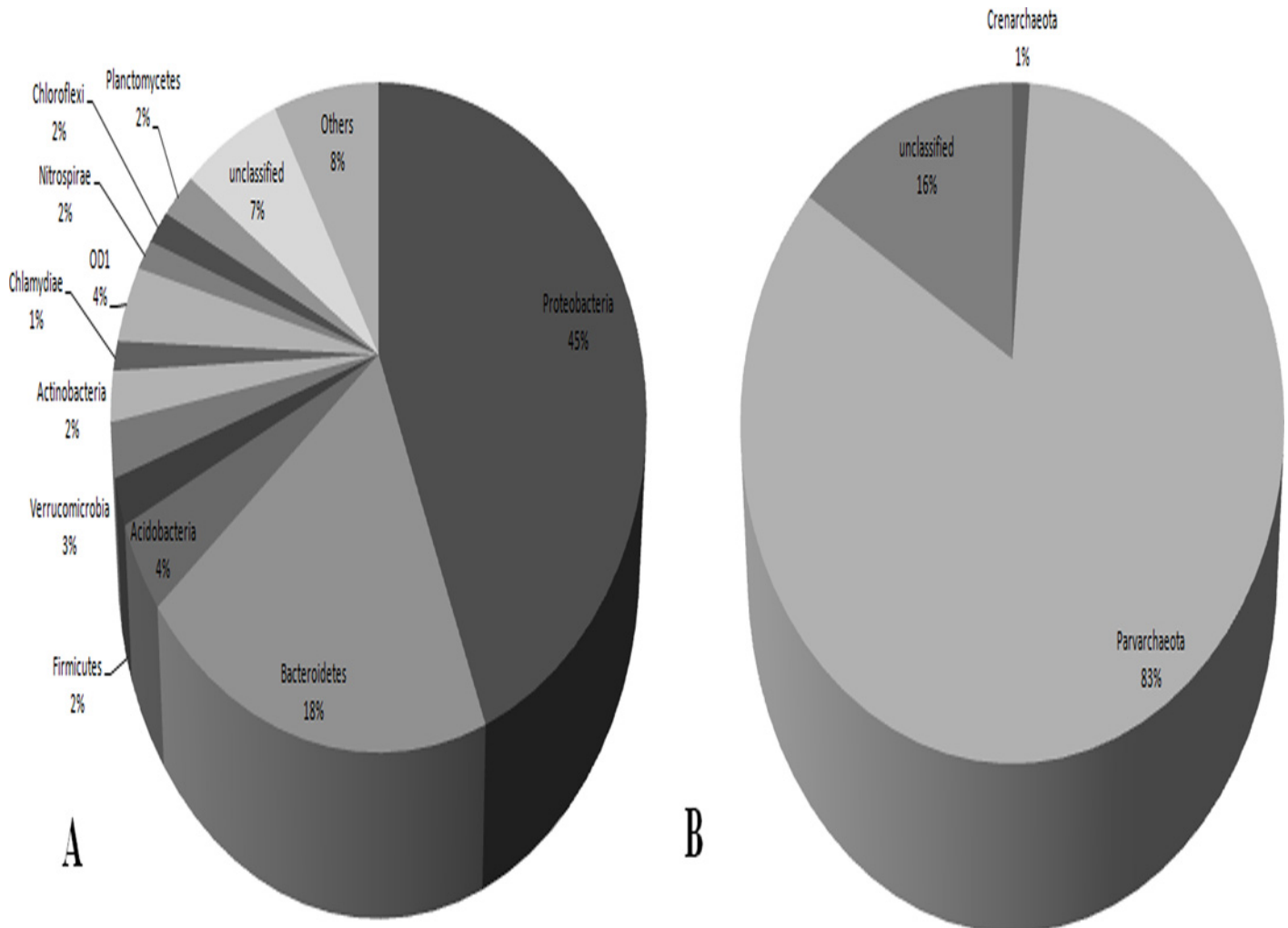


Fig 1. Bacterial and archaeal phyla abundance. Taxonomic composition of bacterial (A) and archaeal (B) taxa from MSS microbiota based on the Greengenes database. Other bacteria: *Gemmatimonadetes*, *Cyanobacteria*, *OP3*, *OP11*, *Spirochaetes*, *TM7*, *Chlorobi*, *WS3*, *Elusimicrobia*, *GN04*, *TM6*, *GN02*, *Tenericutes*, *Armatimonadetes*, *BRC1*, *NC10*, *WPS-2*, *Fibrobacteres*, *Fusobacteria*, *H-178*, *FCPU426*, *Kazan-3B-28*, *WS5*, *NKB19*, *Thermi*, *AC1*, *TPD-58*, *WS6*, *Synergistetes*, *OP8*, *WS2*, *ZB3*, *SC4*, *OP1*, *SBR1093*, *SR1*, *Lentisphaerae*, *GAL15*, *PAUC34f*, *LCP-89* and *MVS-104*.

doi:10.1371/journal.pone.0119465.g001

All proteobacterial classes were represented, with the *Beta*-, *Gamma*-, and *Deltaproteobacteria* classes being the most abundant (81%). *Bacteroidetes* were identified primarily as members of the *Sphingobacteria* (53%), *Flavobacteria* (17%), *Bacteroidia* (17%) and incertae sedis (13%) classes. The *Acidobacteria* phylum was represented by 19 classes, with Gp6, Gp17, Gp3 and *Holophagae* accounting for 69% of representation.

Only 8,430 OTUs (26.6%) were classified at the genus level. The predominant genera observed were, *Sediminibacterium* (*Bacteroidetes*, 520 OTUs), *Flavobacterium* (*Bacteroidetes*, 392), *Prevotella* (*Bacteroidetes*, 371), *Geobacter* (*Proteobacteria*, 323), *Nitrospira* (*Nitrospirae*, 303), *Haliscomenobacter* (*Bacteroidetes*, 250), *Thermomonas* (*Proteobacteria*, 245), *Thiobacillus* (*Proteobacteria*, 240), *Acinetobacter* (*Proteobacteria*, 222) and *Acidovorax* (*Proteobacteria*, 200).

Recruitment of MSS metagenome contigs by bacterial genomes are illustrated in Fig. 2 and S2A-G Figs. The bacterial genome that recruited the majority of the contigs was *Candidatus Nitrospira defluvii* (Fig. 2A and B). Other bacterial species were also reasonably well recruited,

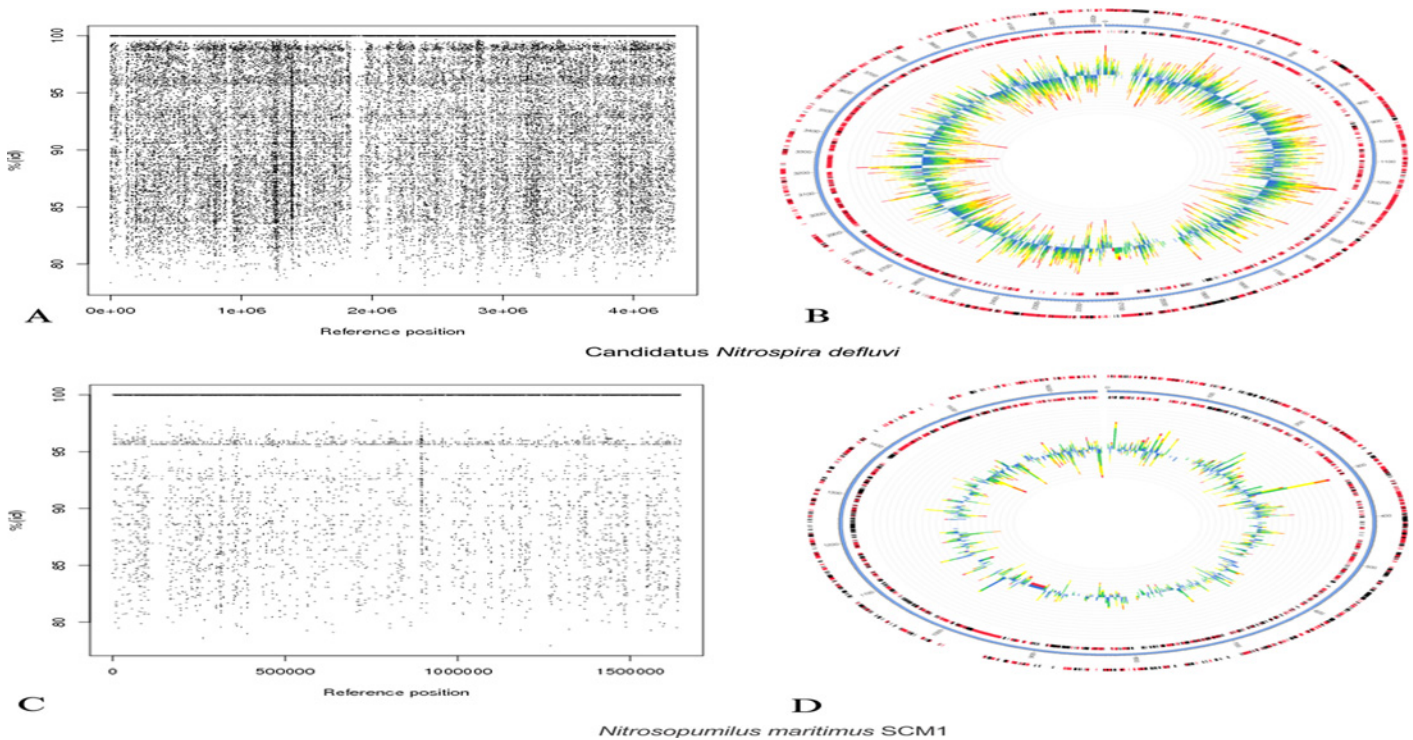


Fig 2. Fragment recruitment plots of the MSS contigs. *Candidatus Nitrospira defluvi* (A and B—FP929003.1) and *Nitrosopumilus maritimus* (C and D—CP000866.1). The comparison was made using BLASTn. Vertical axis showed the % identity of the metagenomic contigs to the respective bacterial or archaeal genome. A and C—recruitment by R software; B and D—recruitment by MG-RAST.

doi:10.1371/journal.pone.0119465.g002

such as *Anaeromyxobacter dehalogenans*, *Chitinophaga pinensis* DSM2588, *Geobacter metallireducens*, *Leptothrix chlolodnii*, *Sideroxydans lithotrophicus*, *Thiobacillus denitrificans*, and *Thiomonas* 3As (S2 Fig.).

The taxonomic affiliation of the Archaea domain revealed that most of the OTUs belonged to the *Parvarchaeota* phylum (83%) represented by the *Parvarchaea* (83%) and *Micrarchaea* (17%) classes. The *Crenarchaeota* phylum (1%) was also represented by three OTUs related to the Miscellaneous Crenarchaeotal Group (MCG). Although members of the *Thaumarchaeota* phylum were not identified in the MSS microbiota, it was possible to recruit the partial genome of three *Thaumarchaeota* species: *Nitrosopumilus maritimus* SCM1, an ammonia oxidizing archaea belonging to the *Nitrosopumilaceae* family that was originally isolated from a marine fish tank [31] (Fig. 2C and D); *Cenarchaeum symbiosum*, a psychrophilic archaea species that belongs to *Cenarchaeaceae* family and inhabits a marine sponge; and *Candidatus Nitrososphaera gargensis*, an ammonia oxidizing species from *Nitrososphaeraceae* family (S2H-I Figs.).

Abundance of the bacteria and Archaea domains

The absolute quantification of bacterial and archaeal communities by qPCR was accomplished and generated R^2 values of 0.99 for both curves and slopes of -3.23 and -3.35, respectively (S3A-D Figs.). According to qPCR analysis, the bacterial 16S rRNA gene copy number (7.7×10^6 gene copies g^{-1}) was two orders of magnitude higher than the archaeal, with 5.3×10^4 gene copies g^{-1} in the sediment sample (S4A and B Figs.).

Overview of metagenomic data

Random shotgun metagenome sequencing from MSS resulted in 158,882,631 reads (50 bp per read) totaling a ~7.9 Gbp dataset. Assembly of reads by Metavelvet resulted in 378,588 contigs ranging from 60 to 2911 bp. After being trimmed by MG-RAST based on quality, size, and artificial removal of duplicate reads, a total of 350,111 clean contigs were used for further analysis. The contig dataset was used to determine the functional analysis. The MSS metagenome exhibited a wide range of GC content from 15% to 80%. Most of the contigs were grouped and ranged from 40 to 60% GC content, with an average GC content of $45 \pm 8\%$.

SEED and KEGG analyses with MG-RAST

Of the 350,111 contigs analyzed for the functional annotation based on the SEED subsystem classification (MG-RAST), 135,632 contigs (39%) could be assigned to functional categories, i.e., predicted proteins with known functions. Nevertheless, most of the contigs (53%) were related to predicted proteins with unknown function, whereas the remaining contigs (8%) presented no match with the SEED database.

Twenty-eight functional subsystems were identified in the MSS metagenome. Protein metabolism, clustering-based subsystems, miscellaneous, carbohydrates, and RNA metabolism presented the largest number of annotated contigs. Other subsystems were related to mobile elements (phages, transposons, integrons, plasmids, and pathogenicity islands) (4%) and stress response (3%), both of which are involved in the fast response and adaptation of the microbial community to changes in the environment (Fig. 3).

Functional analysis with the KEGG Mapper tool of the MG-RAST allows an integrated view of the environmental global metabolism. Assignment of the MSS contigs revealed that most of the metabolic pathways were detected (data not shown). The metabolic pathways identified in the KEGG database as the most abundant were carbohydrate, amino acids, and energy metabolic pathways, indicating that microbial communities inhabiting the MSS are well adapted to degrade carbon substrates such as soluble carbohydrates or polysaccharides and amino acid and derivatives.

Among the genes detected in the MSS, we focused our SEED and KEGG analyses on metal resistance and nitrogen metabolism, which might have particular importance for this environment.

Nitrogen metabolism analysis

The Mina Stream is a eutrophic water body presenting high nitrogen concentration and of its inorganic forms [11]. Therefore, nitrogen metabolism was analyzed, and revealed the presence of enzymes that play a role in ammonia assimilation (49%), nitrate and nitrite ammonification (33%), allantoin utilization (7%), nitrogen fixation (5%), nitric oxide synthase (3%), and cyanate hydrolysis (3%). Relevant genes involved in these six processes revealed by SEED and KEGG databases are displayed in Table 1 and S5 Figs.

Metal resistance analysis

The genes associated with heavy metals were highly diverse, with cobalt-zinc-cadmium (47%) and copper resistance (30%) being the most abundant, followed by the arsenic resistance genes accounting for 6% (Table 1). Interestingly, the presence of the *arsC* resistance gene was not detected in the MSS metagenome even though this gene is the most widespread arsenic resistance gene in the environment [32].

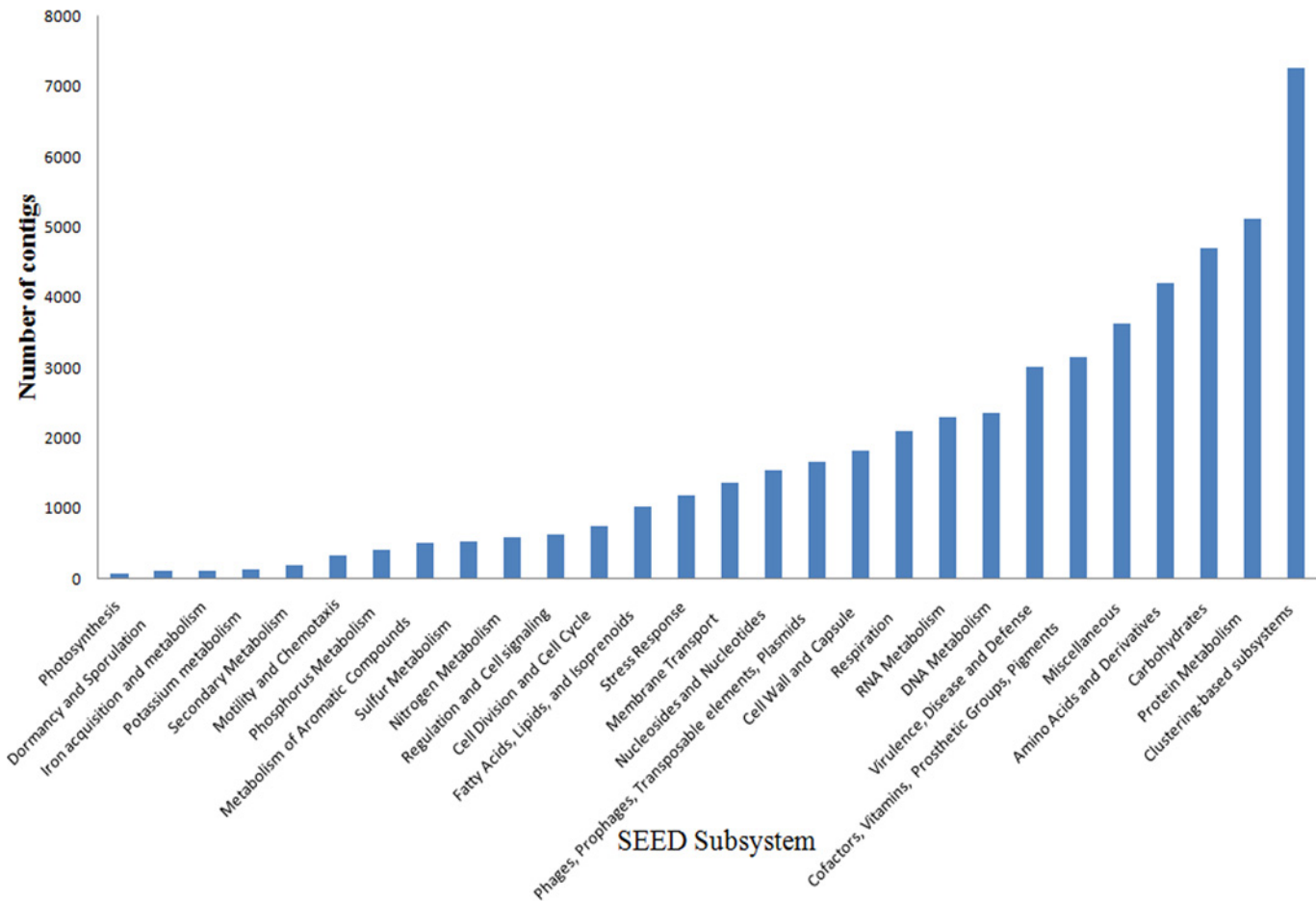


Fig 3. SEED subsystems distribution of the MSS metagenome based on MG-RAST annotation. The cutoff parameters were e-value 1×10^{-5} and 60% of identity.

doi:10.1371/journal.pone.0119465.g003

Statistical comparison of As-contaminated environment

Statistical comparison of the SEED subsystem resemblances between two or more environments can reveal enriched subsystems for a particular environment. To determine biologically significant differences, the functional subsystems detected in the MSS metagenome were statistically compared with the RAW metagenome, as described by Mailloux *et al.* [17]. SEED subsystem comparison revealed a high degree of similarity between the MSS and RAW metagenomes (Fig. 4). However, some differences were observed with significantly over abundant reads in the MSS, which were assigned to mobile elements, regulation and cell signaling, phosphorus metabolism, virulence and defense subsystems, among others. By contrast, the RAW metagenome identified more reads in the amino acid and derivative, clustering-based, carbohydrates, and subsystems related to cell maintenance (Fig. 4). The two metagenomes, MSS and RAW, statistically differed in the enrichment of contigs related to respiratory arsenate reductase (ArrA and ArrB proteins) and multicopper oxidase, which were more frequent in the MSS. By contrast, the RAW metagenome overrepresented arsenate reductase (ArsC) and copper homeostasis (CutE) proteins in the dataset (Fig. 5).

Table 1. The most frequent nitrogen metabolism and metal resistance proteins in the MSS metagenome obtained using the MG-RAST web server based on SEED database.

	Protein	Number of contigs
Nitrogen Metabolism		
Allantoin Utilization	2-hydroxy-3-oxopropionate reductase (EC 1.1.1.60)	43
	Allantoate amidohydrolase (EC 3.5.3.9)	50
	Ureidoglycolate dehydrogenase (EC 1.1.1.154)	53
Ammonia assimilation	Ammonium transporter	64
	Ferredoxin-dependent glutamate synthase (EC 1.4.7.1)	525
	Glutamate synthase [NADH] (EC 1.4.1.14)	43
	Glutamate synthase [NADPH] large and small chain (EC 1.4.1.13)	123
	Glutamate-ammonia-ligase adenylyltransferase—GlnE (EC 2.7.7.42)	44
	Glutamine synthetase type I and type III (EC 6.3.1.2)	130
Cyanate hydrolysis	Carbonic anhydrase—CynT (EC 4.2.1.1)	44
Nitrate and nitrite ammonification	Assimilatory nitrate reductase large subunit (EC:1.7.99.4)	77
	Nitrite reductase [NAD(P)H] small subunit (EC 1.7.1.4)	30
	Nitrite reductase probable electron transfer 4Fe-S subunit (EC 1.7.1.4)	210
	NrfC protein	51
	Polyferredoxin NapH (periplasmic nitrate reductase)	59
	Putative thiol:disulfide oxidoreductase, nitrite reductase complex assembly	76
	Respiratory nitrate reductase delta chain (EC 1.7.99.4)	42
	Respiratory nitrate reductase subunit, conjectural (EC 1.7.99.4)	78
Nitric oxide synthase	Manganese superoxide dismutase (EC 1.15.1.1)	42
Nitrogen fixation	AnfO protein, required for Mo- and V-independent nitrogenase	51
	Nitrogenase (vanadium-iron) beta chain (EC 1.18.6.1)	47
Metal resistance		
Arsenic resistance	Arsenic resistance operon (ArsB, ArsH, ArsA, ArsR, ArsD)	67
	Arsenical-resistance protein ACR3	112
	Respiratory arsenate reductase, Mo binding subunit and FeS subunit (ArrA and ArrB)	124
Cobalt-zinc-cadmium resistance	Cadmium-transporting ATPase—CRA (EC 3.6.3.3)	24
	Probable cadmium-transporting ATPase—PCT (EC 3.6.3.3)	20
	Cation efflux system protein (CusA, CusR, CusC, CusB)	990
	Cobalt-zinc-cadmium resistance protein (CzcA, CzcD, CzcB, CzcR, CzcB)	2007
	Probable Co/Zn/Cd efflux system membrane fusion protein (CusB/CzsB)	160
	Putative silver efflux pump	45
Copper homeostasis	Copper-translocating P-type ATPase (EC 3.6.3.4)	504
	Cytochrome c heme lyase subunit CcmF	31
	Multicopper oxidase	187
Mercuric reductase	FAD-dependent NAD(P)-disulphide oxidoreductase	85
Mercury resistance operon	Mercuric resistance proteins (MerC, MerE, MerT, MerD, MerR, MerP, MerA)	200
Resistance to chromium compounds	Chromate resistance proteins (ChrI, ChrA, ChrC)	17
Zinc resistance	Response regulator of zinc sigma-54-dependent two-component system (ZraR)	72

doi:10.1371/journal.pone.0119465.t001

Metabolic diversity and community-level physiological profiles (CLPP)

The metabolic profile of the microbial community of the MSS was assessed using Biolog Eco-plate (Biolog, Inc.). Substrate utilization patterns from microbial communities are shown in [S2 Table](#). The highest metabolic diversity was observed under anaerobic conditions (30 carbon sources consumed), whereas the community under aerobic conditions consumed 26 carbon

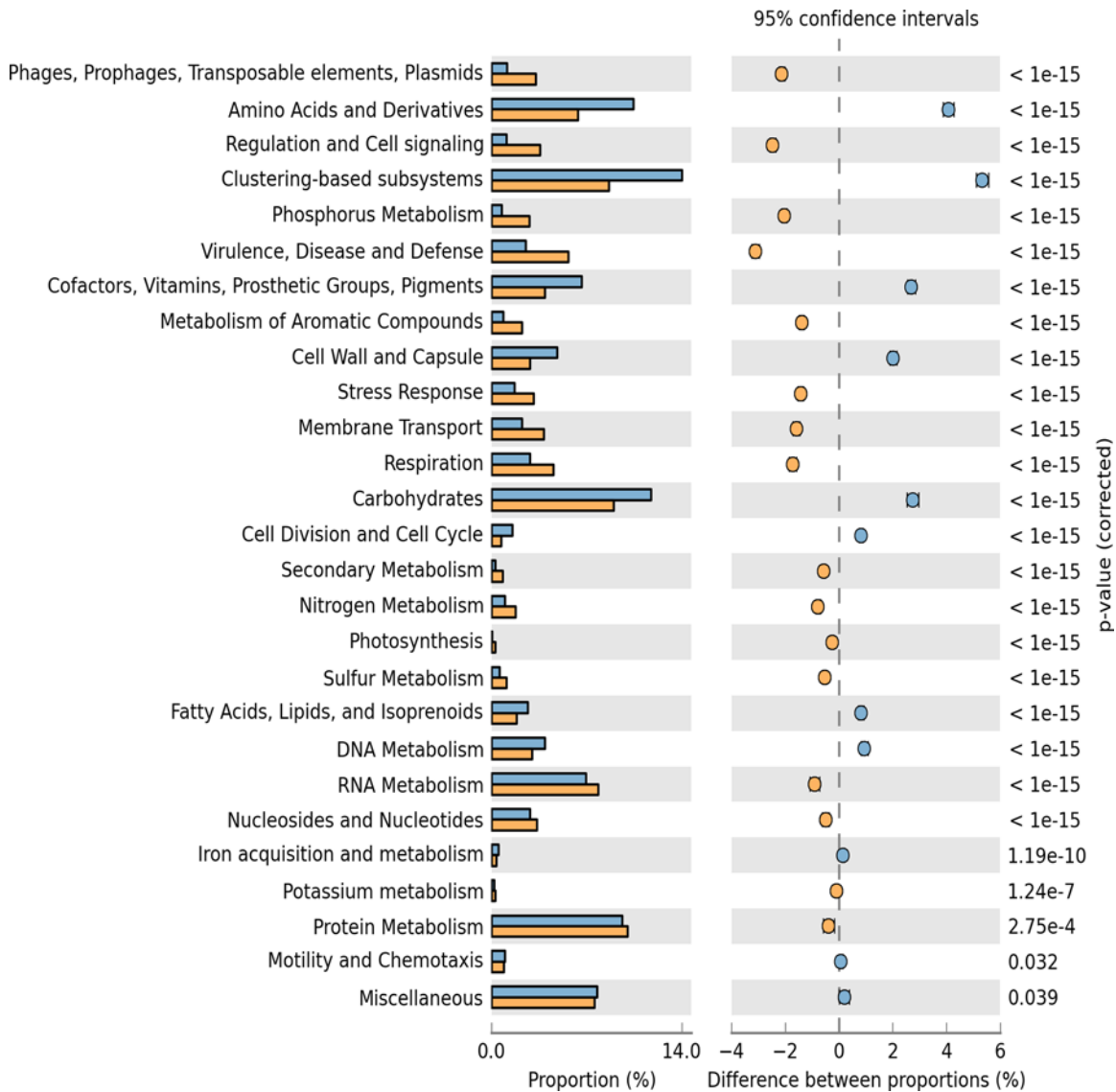


Fig 4. Significant SEED subsystem differences as a result of a Fisher exact test between the MSS and RAW metagenomes conducted with the STAMP program. Enrichment of SEED subsystem in the RAW metagenome has a positive difference between proportions (blue circles), whereas enrichment of SEED subsystem in the MSS metagenome has a negative difference between proportions (orange circles). Bars on the left represent the proportion of each subsystem in the data. Subsystems difference with a *p* value of >0.05 were considered to be significant.

doi:10.1371/journal.pone.0119465.g004

sources. 2-hydroxy benzoic acid was the only carbon source not consumed by either microbial community. The substrates α -ketobutyric acid, L-threonine, glycogen, and α -D-lactose were not consumed by the aerobic microbial community.

AWCD reflects the carbon source utilization ability of the microbial community over time. AWCD analysis showed that the microbial community under anaerobic conditions reached the maximum carbon source utilization at just 72 h, after which time the activity reached a plateau (as demonstrated by the maximum color development). By contrast, the microbial community under aerobic conditions did not reach the maximum color development, showing slower growth and consumption of the carbon source (Fig. 6).

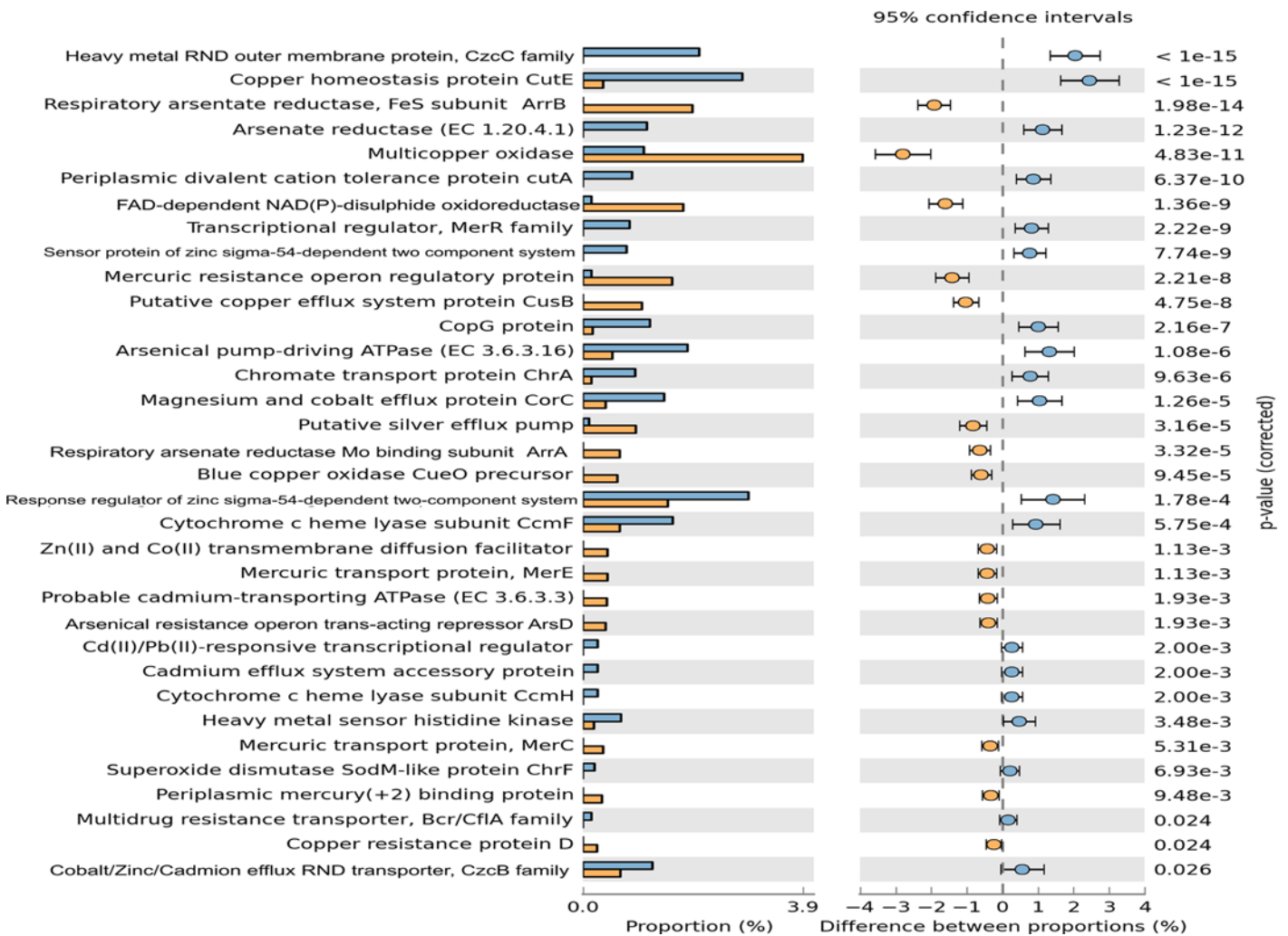


Fig 5. Significant metal resistance genes differences as a result of a Fisher exact test between the MSS and RAW metagenomes conducted with the STAMP program. Enrichment of metal resistance genes in the RAW metagenome has a positive difference between proportions (blue circles), whereas enrichment of metal resistance genes in the MSS metagenome has a negative difference between proportions (orange circles). Bars on the left represent the proportion of each metal resistance protein in the data. Metal resistance difference with a *p* value of >0.05 were considered to be significant.

doi:10.1371/journal.pone.0119465.g005

The Shannon and Simpson diversity indices of the microbial community metabolic profile were calculated, revealing moderate diversity in both communities (S2 Table). Although the anaerobic community presented greater diversity, the differences were not statistically significant ($P \leq 0.05$) (S2 Table). In addition, the Simpson's index of microbial community response showed that a few dominant microbial species were responsible for the metabolic profile of both communities.

Discussion

The microbial community plays an important role in the freshwater environment, especially in stream ecosystems where they are responsible for most of the organic matter decomposition [33]. The dataset presented in this study is the first to taxonomically and functionally characterize the microbial community of a metal-contaminated sediment from a tropical freshwater

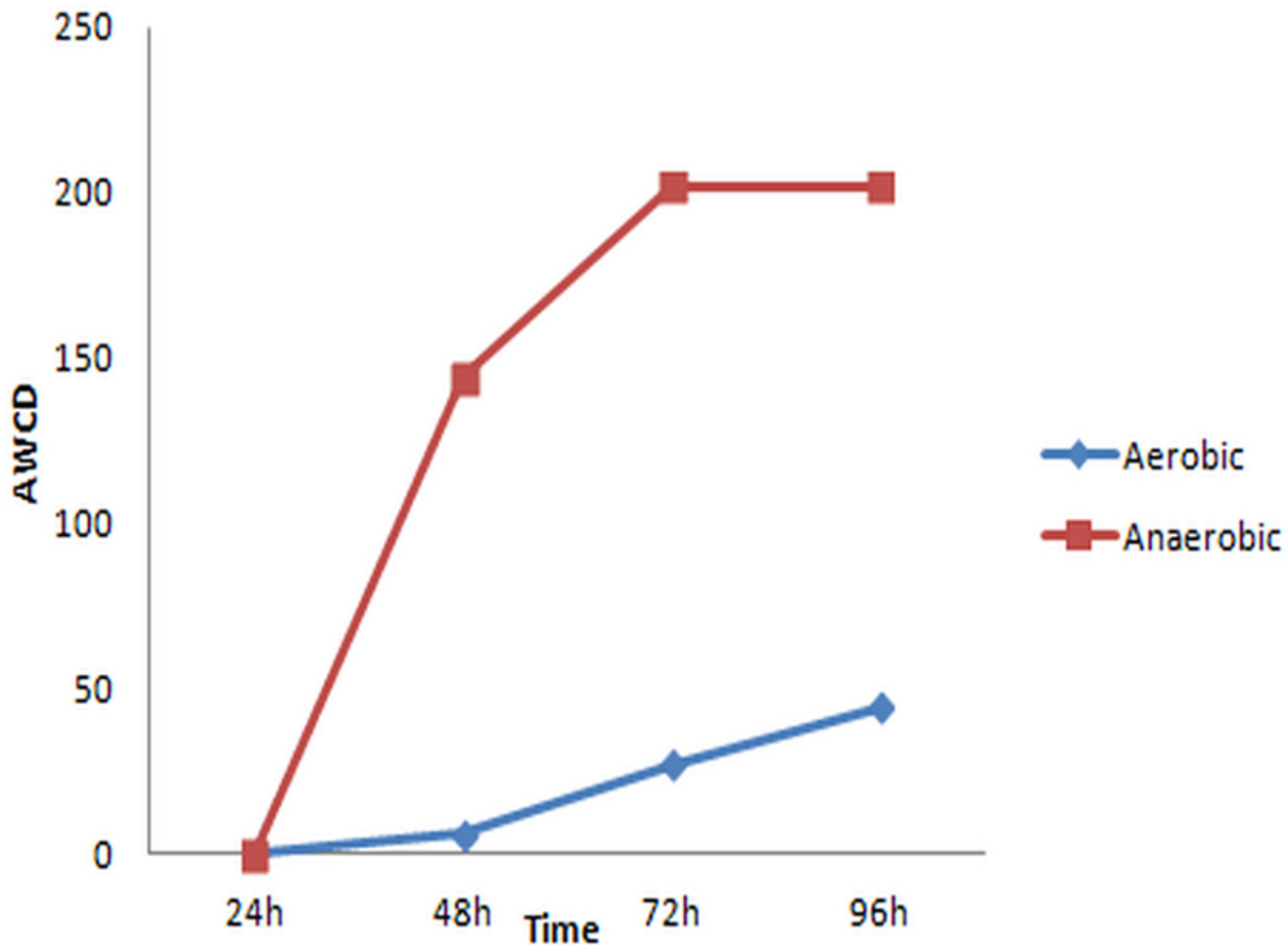


Fig 6. Average well-color development (AWCD) calculated from the consumption of carbon sources of anaerobic and aerobic microbial communities.

doi:10.1371/journal.pone.0119465.g006

stream using a combination of approaches such as metabolic fingerprinting, qPCR, and shotgun metagenomic sequencing.

Taxonomic analyses revealed that a highly complex bacterial community was present in the MSS. Taxonomic data indicated *Proteobacteria* (especially *Beta-proteobacteria*) was the most abundant phylum followed by *Bacteroidetes*. A previous investigation on the prokaryotic diversity in the MSS also showed the predominance of the *Proteobacteria*, but with its classes presenting different tendencies, and *Bacteroidetes* phyla [8]. However, the present study revealed that the bacterial and archaeal 16S rRNA gene copy number was lower in the dry season, in contrast to the increase detected in the rainy season by Reis *et al.* [8]. The observed increase, up to 10 times that of metal concentrations (mainly Zn and As), in the dry season may have affected the cell abundance of the microbial communities present in the MSS, a finding that was reflected in the abundance of the 16S rRNA gene copy number. The eutrophic environment and the presence of high concentrations of metals in the MSS could explain the predominance of *Beta-proteobacteria* and *Bacteroidetes*. Indeed, according to Brümmer *et al.* [33], the predominance of *Beta-proteobacteria* is associated with the presence of high concentrations of ammonia and metals in contaminated water.

Our freshwater tropical sediment results differ from those reported recently for temperate sediments showing that *Proteobacteria* (especially *Deltaproteobacteria*) and *Acidobacteria* were the most abundant phylas [34]. In addition, *Bacteroidetes* were found to be in low proportion in freshwater sediment, albeit enriched when intertidal wetland sediments were analyzed [34]. It should be noted that our data presented a taxonomic similarity with a previous investigation in tropical pristine sediment [8].

Several bacterial species that play an important role in metal contaminated environments were found to inhabit the MSS, as supported by the recruitment plots (Fig. 2 and S2A-E Figs.). The *Beta-proteobacteria* class harbors chemolithoautotrophic members as ferrous iron oxidizing bacteria (FeOB), which were broadly represented in our data [35]. The *Gallionellaceae* family was represented by *Sideroxydans lithotrophicus*, a neutrophilic FeOB that prefers low oxygen and iron-rich environments [7]. *S. lithotrophicus* may play an important role in the removal of As from the MSS environment as FeIII binds with arsenate (AsV), which facilitates its precipitation and decreases its bioavailability in the environment [7]. *Leptothrix cholodnii*, which is often found in eutrophic freshwater environments, was detected in our analysis. This bacterium oxidizes MnII into manganese oxide (MnIII and MnIV) [36, 37]. The *Betaproteobacteria* found in our sample included, among others, *Thiobacillus denitrificans* and *Thiomonas cuprina*. The former oxidizes various reduced inorganic sulfur compounds, such as ferrous sulfide (FeS), coupling with the reduction of nitrate [38, 39]. The latter is an AsIII-oxidizing bacterium that is ubiquitous in arsenic-contaminated environments and is capable of gaining energy from the oxidation of reduced inorganic sulfur compounds (e.g., able to perform the dissimilatory oxidation of iron) [39, 40]. Three FeIII-reducing members of the *Deltaproteobacteria* class were detected. One of them, *Anaeromyxobacter dehalogenans*, is a dissimilatory FeIII-reducing bacterium known to gain energy with Fe reduction [41], a contrasting role to that performed by *Thiomonas cuprina*. The two other members belonged to the *Geobacter* genus and showed the highest abundance among the *Deltaproteobacteria* of the MSS metagenome. Members of this genus were the most recovered in enrichment cultures by FeIII reduction [42]. Altogether, the presence of these taxa may reflect the high concentrations of metals such as Fe, Mn, Cu, As, and Zn found in the MSS. Moreover, the genome of *Chitinophaga pinensis* was well represented in the fragment recruitment plots [43]. This species is associated with organic carbon cycling in both anaerobic and aerobic sediments through the breakdown of simple carbohydrates to organic acids and degradation of a wide range of biopolymers [44, 45].

Members of *Actinobacteria*, *Firmicutes*, and *Nitrospirae* are generally recovered in large proportions from freshwater environments [46, 34], which is in contrast to the present observation for the MSS. Studies suggest that the abundance of the *Actinobacteria* and *Firmicutes* phyla is significantly correlated with metal-contaminated environments, particularly resistance to As and Hg [7, 8, 47, 48]. However, the metal contamination found in MSS does not appear to favor their abundance. Future research will be needed to ascertain the reason for the observed decrease of the abundance of these bacteria in this freshwater sediment and to find whether it is a widespread phenomenon.

The members of the Archaea domain from the MSS belonged to the *Parvarchaeota* and *Crenarchaeota* phyla. The *Crenarchaeota* phylum has been previously described in metal-contaminated environments [7, 49–51]. Our data contrasted with previous studies on archaeal diversity in metal-impacted environments that usually find a predominance of *Crenarchaeota* [8, 52]. The *Parvarchaeota* phylum was recently proposed by Rinke *et al.* [53] from single-cell genome sequencing of an uncultured archaea. *Thaumarchaeota* were represented, only in the metagenomic shotgun sequencing data, by the following ammonium oxidizer species: *Cenarchaeum symbiosum*, *Nitrosopumilus maritimus*, and Candidatus *Nitrosphaera gargensis* [54–56]. Previous investigation on water columns of the Amazon River also detected *Cenarchaeum*

symbiosum and *Nitrosopumilus maritimus*, indicating the importance of these species in the nitrogen (N) cycle of sediment from freshwater environments [50, 57]. It should be noted that the species *Nitrosopumilus maritimus*, detected in the MSS metagenome, showed the highest genome coverage of archaeal reads, indicating that this chemolithoautotrophic nitrifier is globally distributed and is essential for the nitrification mechanisms in this environment.

The presence of various metal resistance genes detected in the MSS metagenome was expected, because the MSS exhibited high concentrations of As, Mn, Zn, and Cu. Despite absence of Co and Cd in MSS, resistance genes associated with cobalt-zinc-cadmium resistance were the most abundant. Resistance determinants to these metals are usually organized as an operon harboring the genes *czcC*, *czcB*, and *czcA*, which are responsible for expression of an efflux pump that transports the ions Co^{+2} , Zn^{+2} , and Cd^{+2} out of the bacterial cell [58, 59]. A previous study investigated the expression of this operon in the presence of these metals separately and found that the expression was more efficient in the presence of high concentrations of Zn [60]. Thus, the high concentration of Zn in the MSS could explain the abundance of these genes in this environment. Moreover, genes that confer resistance to Hg were also found in MSS, despite the low concentration of this metal ($<2.5 \text{ mg kg}^{-1}$ and $<0.1 \text{ mg l}^{-1}$ for sediment and water, respectively). This finding could be due to the fact that the Hg resistance genes are co-selected as they are usually located on plasmids and transposons that harbor other resistance genes, such as resistance to betalactamic antibiotics, kanamycin, tetracycline, and others [61–63].

The Cu resistance gene, the second most abundant in the MSS, may be related to bacterial cell protection mechanisms against high concentrations of this metal found in this environment. Cu is an essential metal for the metabolism of the cell, because it is required as a cofactor for several enzymes [64]. Nevertheless, high concentrations of this metal may be toxic for the bacterial cells that have developed homeostasis mechanisms to ensure appropriate internal concentrations of Cu [65].

The As resistance mechanism most widespread in the environment, performed by the ArsC enzyme, was not detected in the MSS. Interestingly, the other genes of the *ars* operon (*arsA*, *arsB*, *arsD*, *arsH*, *arsR*) were found. The bacterial respiratory arsenate reductase enzymes encoded by the *arrA* and *arrB* genes was abundant in the MSS metagenome. A previous study from our group [11] investigating As resistance genes in the MSS using a metagenomic approach also found that the *arrA* gene was the most diverse As gene in the sample, indicating that this dissimilatory arsenate reduction is the most frequent activity. This microbial reduction is one of the main pathways involved in As mobilization in anoxic environments because release of the most toxic and soluble form of As, AsIII, by reducing Fe- or Mn-oxides may increase the contamination of water bodies [66].

Microbial community physiological profile analysis based on the ability to use different carbon sources has been successfully used to characterize microbial diversity in different environments [67–69]. Xiong *et al.* [70] observed that soil uncontaminated by As showed greater metabolic diversity (C sources consumed) than soil newly contaminated with this metalloid, indicating that the microbial community was affected by this contamination. By contrast, our data showed a high metabolic diversity in the MSS, suggesting that As contamination is most likely not affecting the microbial diversity. Furthermore, other studies also reported that high nutrient concentrations in metal-contaminated sediments promote prokaryotic diversity [5, 71].

In freshwater ecosystems, phosphorus (P) and N are limiting nutrients, i.e., variation of these nutrient concentrations limits biological productivity. These nutrients were previously found in various organic and inorganic forms, and their bioavailability to higher trophic levels occurred through microbial transformations, because the organisms used them for growth and, in some cases, as an energy source [72].

The major transformations of N are N fixation, nitrification, denitrification, anammox, and ammonification, all highly dependent on the activities of a diverse assemblage of microorganisms such as bacteria, archaea, and fungi [73, 74]. In addition to metal contamination, Mina Stream is considered to be a eutrophic water body containing high concentrations of total N and its inorganic forms, nitrate (NO_3^- -N, $3103.8 \mu\text{g l}^{-1}$) and ammonium (NH_4^+ -N, $829.5 \mu\text{g l}^{-1}$). Thus, it is likely that several bacterial and archaeal species related to the N cycle, such as *Thiobacillus denitrificans*, *Candidatus Nitrospira defluvii*, *Cenarchaeum symbiosum*, *Nitrosopumilus maritimus*, and *Candidatus Nitrosphaera gargensis*, among others, may play important roles in the N metabolism of the MSS. *Candidatus Nitrospira defluvii* was highly abundant in the MSS metagenome, being the bacterial genome with the highest coverage. These bacterial species are the dominant nitrite-oxidizing species in wastewater treatment plants and have already been found in metal-contaminated sediments [7, 75].

Analysis of N cycling genes from the MSS metagenome unveiled ammonium assimilation and ammonification as the two most abundant N cycle processes. Indeed, genes responsible for ammonium assimilation such as glutamate synthase (EC 1.4.1.13 and EC 1.4.1.14) and glutamine synthetase type I and type III (EC 6.3.1.2) were detected in our samples. Ammonium assimilation performed by the microbial community can retain N and make the sediment act as a temporary buffer in aquatic environments [76, 77]. The ammonification process is performed by saprophytic bacteria and is based on the decomposition of organic molecules containing N, e.g., amino acids and DNA that are released into the environment when an organism excretes waste or dies. N is required for the survival of all organisms, because it is an essential component of DNA, RNA, and protein, and thus, is essential for the maintenance of the aquatic microbial community. As most N exists in the form of organic molecules, the availability of N to higher trophic levels depends on microbial transformation.

In conclusion, our data reveal that the microbial communities from the MSS have significantly different features than those presented by other metal-contaminated environments. The data recovered agree with the expected assemblage of organisms thriving in metal-rich and eutrophic environments. This study provides important insights into the structure of the prokaryotic community of a tropical freshwater sediment, indicating a possible role for this community in the N and C cycles and in the transformation of Fe and As. Functional annotation unveiled a high degree of diversity of several metal resistance genes, indicating that this microbial community is well adapted to environments containing metal contamination. Finally, the results reported here expand the current knowledge of the microbial taxonomic and functional composition of tropical, metal-contaminated, freshwater sediments. Our data, together with those revealed by many other research efforts across the globe, may be an indirect and yet relevant contribution to the enormous endeavor being championed by the Earth microbiome project.

Supporting Information

S1 Fig. Rarefaction curve. Rarefaction curve of number of OTUs observed with an evolutionary distance of 0.03, 0.05 and 0.10. (TIF)

S2 Fig. Fragment recruitment plots of the MSS contigs by bacterial and archaeal genomes. The comparison was made using BLASTn. Vertical axis showed the % identity of the metagenomic contigs to the respective bacterial or archaeal genome. A—*Anaeromyxobacter dehalogenans* 2CP-1 (CP000251.1); B—*Chitinophaga pinensis* DSM2588 (CP001699.1); C—*Geobacter metallireducens* (CP000148.1); D—*Leptothrix chlolodnii* (CP001013.1); E—*Sideroxydans lithotrophicus* (CP001965.1); F—*Thiobacillus denitrificans* ATCC25259 (CP000116.1); G—*Thiomonas*

arsenitoxydans 3As (FP475956.1); H—*Candidatus Nitrososphaera gargensis* (CP002408.1); I—*Cenarchaeum symbiosum* (DP000238.1).

(TIF)

S3 Fig. The bacterial (A and B) and archaeal (C and D) standard curves (A).

(TIF)

S4 Fig. The C_t values from the 16S rRNA gene amplifications. A and B represent bacterial and archaeal amplifications, respectively.

(TIF)

S5 Fig. Nitrogen cycle representation obtained in the Keeg Mapper analysis of MG RAST web server based on SEED database. The red square represents the presence of enzyme sequence in the MSS metagenome.

(TIF)

S1 Table. Taxonomic affiliation of 16S rRNA gene OTUs based on Greengenes database.

(XLSX)

S2 Table. Carbon sources utilization by microbial communities in aerobic and anaerobic condition and diversity index in sediment of the Mina stream.

(DOCX)

Author Contributions

Conceived and designed the experiments: AMAN PSC ECS. Performed the experiments: PSC ACMS FMGA MPR FB. Analyzed the data: AMAN PSC MPR MPÁ LRL. Contributed reagents/materials/analysis tools: AMAN GO. Wrote the paper: AMAN ECS PSC LRL.

References

1. Kasting JF, Siefert JL. Life and the evolution of Earth's atmosphere. *Science*. 2002; 296: 1066–1068. PMID: [12004117](#)
2. Xu J. Microbial ecology in the age of metagenomics. In: Bruijn J, Willey J. *Handbook of Molecular Microbial Ecology I: Metagenomics and Complementary Approaches*; 2011.
3. Earth Microbiome Project. Available: <http://www.earthmicrobiome.org>.
4. Lozupone CA, Knight R. Global patterns in bacterial diversity. *PNAS*. 2007; 104: 11436–11440. PMID: [17592124](#)
5. Bouskill NJ, Barker-Finkel J, Galloway TS, Handy RD, Ford TE. Temporal bacterial diversity associated with metal-contaminated river sediments. *Ecotoxicol*. 2010; 19: 317–328.
6. Rezende PS, Moura PAS, Durão WA Jr, Nascentes CC, Windmüller CC, Costa LM. Arsenic and mercury mobility in Brazilian sediments from the São Francisco River Basin. *J Braz Chem Soc*. 2011; 22: 910–918.
7. Halter D, Cordi A, Gribaldo S, Gallien S, Goulhen-Chollet F, Heinrich-Salmeron A, et al. Taxonomic and functional prokaryote diversity in mildly arsenic contaminated sediments. *Res Microbiol*. 2011; 162: 1–11. doi: [10.1016/j.resmic.2010.11.007](#) PMID: [21534268](#)
8. Reis MP, Barbosa FA, Chartone-Souza E, Nascimento AMA. The prokaryotic community of a historically mining-impacted tropical stream sediment is as diverse as that from a pristine stream sediment. *Extremophiles*. 2013; 17: 301–319. doi: [10.1007/s00792-013-0517-9](#) PMID: [23389654](#)
9. Gillan DC, Roosa S, Kunath B, Billon G, Wattiez R. The long-term adaptation of bacterial communities in metal-contaminated sediments: a metaproteogenomic study. *Environ Microbiol*. 2014; 1–15. doi: [10.1111/1462-2920.12620](#) PMID: [25297499](#)
10. Gough HL, Stahl DA. Microbial community structures in anoxic freshwater lake sediment along a metal contamination gradient. *ISME J*. 2011; 5: 543–58. doi: [10.1038/ismej.2010.132](#) PMID: [20811473](#)

11. Costa PS, Scholte LL, Reis MP, Chaves AV, Oliveira PL, Itabayana LB, et al. Bacteria and genes involved in arsenic speciation in sediment impacted by long-term gold mining. *PLoS One*. 2014; 9: e95655. doi: [10.1371/journal.pone.0095655](https://doi.org/10.1371/journal.pone.0095655) PMID: [24755825](https://pubmed.ncbi.nlm.nih.gov/24755825/)
12. Gilbert JA, Dupont CL. Microbial metagenomics: beyond the genome. *Ann Rev Mar Sci*. 2011; 3: 347–71. PMID: [21329209](https://pubmed.ncbi.nlm.nih.gov/21329209/)
13. Borba RP, Figueiredo BR, Rawlins BG, Matchullat J. Arsenic in water and sediment in the Iron Quadrangle, Minas Gerais state, Brazil. *Rev Brasil Geocienc*. 2000; 30: 554–557.
14. Deschamps E, Ciminelli VST, Raue B, Lange FT, Schmidt H. Soil and sediment geochemistry of the Iron Quadrangle, Brazil. *J Soil Sediment*. 2002; 2: 216–222.
15. Borba RP, Figueiredo BR, Cavalcanti JA. Arsênio na água subterrânea em Ouro Preto e Mariana, Quadrilátero Ferrífero (MG). *R Esc Minas*. 2004; 57: 45–51.
16. Bundschuh J, Litter MI, Parvez F, Román-Ross G, Nicolli HB, Jean JS, et al. One century of arsenic exposure in Latin America: a review of history and occurrence from 14 countries. *Sci Total Environ*. 2012; 429: 2–35. doi: [10.1016/j.scitotenv.2011.06.024](https://doi.org/10.1016/j.scitotenv.2011.06.024) PMID: [21959248](https://pubmed.ncbi.nlm.nih.gov/21959248/)
17. Mailloux BJ, Trembath-Reichert E, Cheung J, Watson M, Stute M, Freyer GA, et al. Advection of surface-derived organic carbon fuels microbial reduction in Bangladesh groundwater. *PNAS*. 2013; 110:5331–5. doi: [10.1073/pnas.1213141110](https://doi.org/10.1073/pnas.1213141110) PMID: [23487743](https://pubmed.ncbi.nlm.nih.gov/23487743/)
18. Garland JL, Mills AL. Classification and characterization of heterotrophic microbial communities on the basis of patterns of community-level sole-carbon-source utilization. *Appl Environ Microbiol*. 1991; 57:2351–2359. PMID: [16348543](https://pubmed.ncbi.nlm.nih.gov/16348543/)
19. Garland JL. Analysis and interpretation of community-level physiological profiles in microbial ecology. *FEMS Microbiol Ecol*. 1996; 24: 289–300
20. Klindworth A, Pruesse E, Schweer T, Peplens J, Quast C, et al. Evaluation of general 16S ribosomal RNA gene PCR primers for classical and next-generation sequencing-based diversity studies. *Nucleic Acids Res*. 2013; 41:1–11. doi: [10.1093/nar/gks1039](https://doi.org/10.1093/nar/gks1039) PMID: [23143271](https://pubmed.ncbi.nlm.nih.gov/23143271/)
21. Mothur Pipeline MiSeq Sop. Available: http://www.mothur.org/wiki/MiSeq_SOP-20-07-2014.
22. Drancourt M, Bollet C, Carlioz A, Martelin R, Gayral J-P, Raoult D. 16S Ribosomal DNA sequence analysis of a large collection of environmental and clinical unidentifiable bacterial isolates. *J Clin Microbiol*. 2000; 34:3623–3630.
23. Good IJ. The population frequencies of species and the estimation of population parameters. *Biometrika*. 1953; 40:237–262.
24. Namiki T, Hachiya T, Tanaka H, Sakakibara Y. MetaVelvet: an extension of Velvet assembler to de novo metagenome assembly from short sequence reads. *Nucleic Acids Res*. 2012; 1:e155.
25. Meyer F, Paarmann D, D'Souza M, Olson R, Glass EM, Kubal M, et al. The metagenomics RAST server—a public resource for the automatic phylogenetic and functional analysis of metagenomes. *BMC Bioinformatics*. 2008; 19:386.
26. Mitra S, Rupek P, Richter DC, Urich T, Gilbert JA, Meyer F, et al. Functional analysis of metagenomes and metatranscriptomes using SEED and KEGG. *BMC Bioinformatics*. 2011; 12:1–8. doi: [10.1186/1471-2105-12-1](https://doi.org/10.1186/1471-2105-12-1) PMID: [21199577](https://pubmed.ncbi.nlm.nih.gov/21199577/)
27. Parks DH, Beiko RG. Identifying biologically relevant differences between metagenomic communities. *Bioinformatics*. 2010; 26: 715–721. doi: [10.1093/bioinformatics/btq041](https://doi.org/10.1093/bioinformatics/btq041) PMID: [20130030](https://pubmed.ncbi.nlm.nih.gov/20130030/)
28. Raskin L, Stromley JM, Rittmann BE, Stahl DA. Group-specific 16S rRNA hybridization probes to describe natural communities of methanogens. *Appl Environ Microbiol*. 1994; 60: 1232–1240. PMID: [7517128](https://pubmed.ncbi.nlm.nih.gov/7517128/)
29. Muyzer G, De Waal EC, Uitterlinden AG. Profiling of complex microbial populations by denaturing gradient gel electrophoresis analysis of polymerase chain reaction-amplified genes coding for 16S rRNA. *Appl Environ Microbiol*. 1993; 59: 695–700. PMID: [7683183](https://pubmed.ncbi.nlm.nih.gov/7683183/)
30. Cardinali-Rezende J, Colturato LF, Colturato TD, Chartone-Souza E, Nascimento AMA, Sanz JL. Prokaryotic diversity and dynamics in a full-scale municipal solid waste anaerobic reactor from start-up to steady-state conditions. *Bioresour Technol*. 2012; 119: 373–83. doi: [10.1016/j.biortech.2012.05.136](https://doi.org/10.1016/j.biortech.2012.05.136) PMID: [22750748](https://pubmed.ncbi.nlm.nih.gov/22750748/)
31. Könneke M, Bernhard AE, de la Torre JR, Walker CB, Waterbury JB, Stahl DA. Isolation of an autotrophic ammonia-oxidizing marine archaeon. *Nature*. 2005; 437:543–6. PMID: [16177789](https://pubmed.ncbi.nlm.nih.gov/16177789/)
32. Liao VH, Chu Y, Su Y, Hsiao S, Wei C, Liu C, et al. Arsenite-oxidizing and arsenate-reducing bacteria associated with arsenic-rich groundwater in Taiwan. *J Contam Hydrol*. 2011; 123: 20–9. doi: [10.1016/j.jconhyd.2010.12.003](https://doi.org/10.1016/j.jconhyd.2010.12.003) PMID: [21216490](https://pubmed.ncbi.nlm.nih.gov/21216490/)

33. Brümmer IH, Fehr W, Wagner-Dobler I. Biofilm community structure in polluted rivers: abundance of dominant phylogenetic groups over a complete annual cycle. *Appl Environ Microbiol.* 2000; 66: 3078–3082. PMID: [10877809](#)
34. Wang Y, Sheng HF, He Y, Wu JY, Jiang YX, Tam NF, et al. Comparison of the levels of bacterial diversity in freshwater, intertidal wetland, and marine sediments by using millions of illumina tags. *Appl Environ Microbiol.* 2012; 78:8264–8271. doi: [10.1128/AEM.01821-12](#) PMID: [23001654](#)
35. Hedrich S, Schlömann M, Johnson DB. The iron-oxidizing proteobacteria. *Microbiology.* 2011; 157:1551–1564. doi: [10.1099/mic.0.045344-0](#) PMID: [21511765](#)
36. Tebo BM, Johnson HA, McCarthy JK, Templeton AS. Geomicrobiology of manganese(II) oxidation. *Trends Microbiol.* 2005; 13: 421–8. PMID: [16054815](#)
37. Takeda M, Kawasaki Y, Umezumi T, Shimura S, Hasegawa M, Koizumi J. Patterns of sheath elongation, cell proliferation, and manganese(II) oxidation in *Leptothrix cholodnii*. *Arch Microbiol.* 2012; 194: 667–73. doi: [10.1007/s00203-012-0801-6](#) PMID: [22392226](#)
38. Jørgensen CJ, Jacobsen OS, Elberling B, Aamand J. Microbial oxidation of pyrite coupled to nitrate reduction in anoxic groundwater sediment. *Environ Sci Technol.* 2009; 43: 4851–4857. PMID: [19673275](#)
39. Hedrich S, Schlömann M, Johnson DB. The iron-oxidizing proteobacteria. *Microbiology.* 2011; 157: 1551–1564. doi: [10.1099/mic.0.045344-0](#) PMID: [21511765](#)
40. Bryan CG, Marchal M, Battaglia-Brunet F, Kugler V, Lemaitre-Guillier C, Lièvreumont D, et al. Carbon and arsenic metabolism in *Thiomonas* strains: differences revealed diverse adaptation processes. *BMC Microbiol.* 2009; 23: 127.
41. Truede N, Rosencrantz D, Liesack W, Schnell S. Strain Fac12, a dissimilatory iron-reducing member of the *Anaeromyxobacter* subgroup of Myxococcales. *FEMS Microbiol Lett.* 2003; 44: 261–269.
42. Snoeyenbos-West O, Nevin KP, Anderson RT, Lovley DR. Enrichment of *Geobacter* species in response to stimulation of Fe(III) reduction in sandy aquifer sediments. *Microbiol Ecol.* 2000; 39: 153–167. PMID: [10833228](#)
43. Del Rio TG, Abt B, Spring S, Lapidus A, Nolan M, Tice H, et al. Complete genome sequence of *Chitinophaga pinensis* type strain (UQM 2034T). *Stand Genomic Sci.* 2010; 2: 87–95. doi: [10.4056/signs.661199](#) PMID: [21304681](#)
44. Pankratov TA, Kulichevskaya IS, Liesack W, Dedysh SN (2006) Isolation of aerobic, gliding, xylanolytic and laminarinolytic bacteria from acidic Sphagnum peatlands and emended description of *Chitinophaga arvensicola* Kampf et al. 2006. *Int J Syst Evol Microbiol* 56: 2761–4. PMID: [17158974](#)
45. Briée C, Moreira D, López-García P. Archaeal and bacterial community composition of sediment and plankton from a suboxic freshwater pond. *Res Microbiol.* 2007; 158: 213–27. PMID: [17346937](#)
46. Newton RJ, Jones SE, Eiler A, McMahon KD, Bertilsson S. A guide to the natural history of freshwater lake bacteria. *Microbiol Mol Biol Rev.* 2011; 75: 14–49. doi: [10.1128/MMBR.00028-10](#) PMID: [21372319](#)
47. Gremion F, Chatzinotas A, Harms H. Comparative 16S rDNA and 16S rRNA sequence analysis indicates that Actinobacteria might be a dominant part of the metabolically active bacteria in heavy metal-contaminated bulk and rhizosphere soil. *Environ Microbiol.* 2003; 5: 896–907. PMID: [14510843](#)
48. Vishnivetskaya TA, Mosher JJ, Palumbo AV, Yang ZK, Podar M, Brown SD, et al. Mercury and other heavy metals influence bacterial community structure in contaminated Tennessee streams. *Appl Environ Microbiol.* 2011; 77: 302–311. doi: [10.1128/AEM.01715-10](#) PMID: [21057024](#)
49. Bruneel O, Pascault N, Egal M, Bancon-Montigny C, Goni-Urriza MS, Elbaz-Poulichet F, et al. Archaeal diversity in a Fe-As rich acid mine drainage at Carnoules (France). *Extremophiles.* 2008; 12: 563–571. doi: [10.1007/s00792-008-0160-z](#) PMID: [18418543](#)
50. Porat I, Vishnivetskaya TA, Mosher JJ, Brandt CC, Yang ZK, Brooks SC, et al. Characterization of archaeal community in contaminated and uncontaminated surface stream sediments. *Microb Ecol.* 2010; 60: 784–95. doi: [10.1007/s00248-010-9734-2](#) PMID: [20725722](#)
51. Haller L, Tonolla M, Zopfi J, Peduzzi R, Wildi W, Poté J. Composition of bacterial and archaeal communities in freshwater sediments with different contamination levels (Lake Geneva, Switzerland). *Water Res.* 2011; 45: 1213–28. doi: [10.1016/j.watres.2010.11.018](#) PMID: [21145090](#)
52. Gupta RS, Shami A. Molecular signatures for the Crenarchaeota and the Thaumarchaeota. *Antonie van Leeuwenhoek.* 2011; 99: 133–157. doi: [10.1007/s10482-010-9488-3](#) PMID: [20711675](#)
53. Rinke C, Schwientek P, Sczyrba A, Ivanova NN, Anderson IJ, Cheng JF, et al. Insights into the phylogeny and coding potential of microbial dark matter. *Nature.* 2013; 499:431–7. doi: [10.1038/nature12352](#) PMID: [23851394](#)
54. Brochier-Armanet C, Boussau B, Gribaldo S, Forterre P. Mesophilic Crenarchaeota: proposal for a third archaeal phylum, the Thaumarchaeota. *Nat Rev Microbiol.* 2008; 6: 245–52. doi: [10.1038/nrmicro1852](#) PMID: [18274537](#)

55. Spang A, Hatzenpichler R, Brochier-Armanet C, Rattei T, Tischler P, Spieck E, et al. Distinct gene set in two different lineages of ammonia-oxidizing archaea supports the phylum Thaumarchaeota. *Trends Microbiol.* 2010; 18: 331–40. doi: [10.1016/j.tim.2010.06.003](https://doi.org/10.1016/j.tim.2010.06.003) PMID: [20598889](https://pubmed.ncbi.nlm.nih.gov/20598889/)
56. Tourna M, Stieglmeier M, Spang A, Könneke M, Schintlmeister U, Urich, et al. *Nitrososphaera viennensis*, an ammonia oxidizing archaeon from soil. *PNAS.* 2011; 108: 8420–5. doi: [10.1073/pnas.1013488108](https://doi.org/10.1073/pnas.1013488108) PMID: [21525411](https://pubmed.ncbi.nlm.nih.gov/21525411/)
57. Ghai R, Rodriguez-Valera F, McMahon KD, Toyama D, Rinke, Oliveira SC, et al. Metagenomics of the water column in the pristine upper course of the Amazon river. *PLoS One.* 2011; 6: e23785. doi: [10.1371/journal.pone.0023785](https://doi.org/10.1371/journal.pone.0023785) PMID: [21915244](https://pubmed.ncbi.nlm.nih.gov/21915244/)
58. Nies DH, Brown N. Two-component systems in the regulation of heavy metal resistance. In: Silver S, Walden W, editors. *Metal ions in gene regulation.* Chapman & Hall, London, England; 1997.
59. Nies DH, Rehbein G, Hoffmann T, Baumann C, Grosse C. Paralogs of genes encoding metal resistance proteins in *Cupriavidus metallidurans* strain CH34. *J Mol Microbiol Biotechnol.* 2006; 11:82–93. PMID: [16825791](https://pubmed.ncbi.nlm.nih.gov/16825791/)
60. Legatzki A, Grass G, Anton A, Rensing C, Nies DH. Interplay of the Czc system and two P-type ATPases in conferring metal resistance to *Ralstonia metallidurans*. *J Bacteriol.* 2003; 185: 4354–4361. PMID: [12867443](https://pubmed.ncbi.nlm.nih.gov/12867443/)
61. Silver S, Phung LT. Genes and enzymes involved in bacterial oxidation and reduction of inorganic arsenic. *Appl Environ Microbiol.* 2005; 71: 599–608. PMID: [15691908](https://pubmed.ncbi.nlm.nih.gov/15691908/)
62. Soge OO, Beck NK, White TM, No DB, Roberts MC. A novel transposon, Tn6009, composed of a Tn916 element linked with a *Staphylococcus aureus* mer operon. *J Antimicrob Chemother.* 2008; 62: 674–80. doi: [10.1093/jac/dkn255](https://doi.org/10.1093/jac/dkn255) PMID: [18583328](https://pubmed.ncbi.nlm.nih.gov/18583328/)
63. Novais A, Baquero F, Machado E, Cantón R, Peixe L, Coque TM. International spread and persistence of TEM-24 is caused by the confluence of highly penetrating enterobacteriaceae clones and an IncA/C2 plasmid containing Tn1696::Tn1 and IS5075-Tn21. *Antimicrob Agents Chemother.* 2010; 54: 825–34. doi: [10.1128/AAC.00959-09](https://doi.org/10.1128/AAC.00959-09) PMID: [19995930](https://pubmed.ncbi.nlm.nih.gov/19995930/)
64. Krupanidhi S, Sreekumar A, Sanjeevi CB. Copper & biological health. *Indian J Med Res.* 2008; 128: 448–61. PMID: [19106440](https://pubmed.ncbi.nlm.nih.gov/19106440/)
65. Solioz M, Abicht HK, Mermod M, Mancini S. Response of gram-positive bacteria to copper stress. *J Biol Inorg Chem.* 2010; 15: 3–14. doi: [10.1007/s00775-009-0588-3](https://doi.org/10.1007/s00775-009-0588-3) PMID: [19774401](https://pubmed.ncbi.nlm.nih.gov/19774401/)
66. Song B, Chyun E, Jaffé PR, Ward BB. Molecular methods to detect and monitor dissimilatory arsenate-respiring bacteria (DARB) in sediments. *FEMS Microbiol Ecol.* 2009; 68:108–17. doi: [10.1111/j.1574-6941.2009.00657.x](https://doi.org/10.1111/j.1574-6941.2009.00657.x) PMID: [19291024](https://pubmed.ncbi.nlm.nih.gov/19291024/)
67. Mondini C, Insam H. Community level physiological profiling as a tool to evaluate compost maturity: a kinetic approach. *Eur J Soil Biol.* 2003; 39:141–148.
68. Cardinali-Rezende J, Moraes AMM, Colturato LFDB, Carneiro EV, Marriel IE, Chartone-Souza E, et al. Phylogenetic and physiological characterization of organic waste-degrading bacterial communities. *World J Microbiol Biotechnol.* 2011; 27: 245–252.
69. Leon C, Campos V, Urrutia R, Mondaca MA. Metabolic and molecular characterization of bacterial community associated to Patagonian Chilean oligotrophic-lakes of quaternary glacial origin. *World J Microbiol Biotechnol.* 2012; 28:1511–21. doi: [10.1007/s11274-011-0953-6](https://doi.org/10.1007/s11274-011-0953-6) PMID: [22805933](https://pubmed.ncbi.nlm.nih.gov/22805933/)
70. Xiong J, Wu L, Tu S, Van Nostrand JD, He Z, Zhou J, et al. Microbial communities and functional genes associated with soil arsenic contamination and the rhizosphere of the arsenic-hyperaccumulating plant *Pteris vittata* L. *Appl Environ Microbiol.* 2010; 76: 7277–7284. doi: [10.1128/AEM.00500-10](https://doi.org/10.1128/AEM.00500-10) PMID: [20833780](https://pubmed.ncbi.nlm.nih.gov/20833780/)
71. Zhou J, Kia B, Treves DS, Wu L-Y, Marsh TL, O'Neill RV, et al. Spatial and resource factors influencing high microbial diversity in soil. *Appl Environ Microbiol.* 2002; 68: 326–334. PMID: [11772642](https://pubmed.ncbi.nlm.nih.gov/11772642/)
72. Barlett MA, Leff LG. The effects of N:P ratio and nitrogen form on four major freshwater bacterial taxa in biofilms. *Can J Microbiol.* 2010; 56: 32–43. doi: [10.1139/w09-099](https://doi.org/10.1139/w09-099) PMID: [20130692](https://pubmed.ncbi.nlm.nih.gov/20130692/)
73. Purkhold U, Pommerening-Roser A, Juretschko S, Schmid MC, Koops HP, Wagner M. Phylogeny of all recognized species of ammonia oxidizers based on comparative 16S rRNA and *amoA* sequence analysis: implications for molecular diversity surveys. *Appl Environ Microbiol.* 2000; 66: 5368–5382. PMID: [11097916](https://pubmed.ncbi.nlm.nih.gov/11097916/)
74. Wuchter C, Abbas B, Coolen MJ, Herfort L, van Bleijswijk J, Timmers, et al. Archaeal nitrification in the ocean. *PNAS.* 2006; 103: 12317–12322. PMID: [16894176](https://pubmed.ncbi.nlm.nih.gov/16894176/)
75. Maixner F, Wagner M, Lückner S, Pelletier E, Schmitz-Esser S, Hace K, et al. Environmental genomics reveals a functional chlorite dismutase in the nitrite-oxidizing bacterium '*Candidatus Nitrospira defluvi*'. *Environ Microbiol.* 2008; 10: 3043–56. doi: [10.1111/j.1462-2920.2008.01646.x](https://doi.org/10.1111/j.1462-2920.2008.01646.x) PMID: [18459973](https://pubmed.ncbi.nlm.nih.gov/18459973/)

76. Dähnke K, Emeis K, Johannsen A, Nagel B. Stable isotope composition and turnover of nitrate in the German Bight. *Mar Ecol Prog Ser.* 2010; 408: 7–18.
77. Dähnke K, Moneta A, Veuger B, Soetaert K, Middelburg JJ. Nitrogen turnover in a tidal flat sediment: assimilation and dissimilation by bacteria and benthic microalgae. *Biogeosciences Discuss.* 2012; 9: 6987–7019.